

## Miniaturized 60-GHz transformer-based balun splitter with isolation and matching performance in 0.18- $\mu\text{m}$ SiGe BiCMOS

ZHANG Da-Wei<sup>1,3\*</sup>, XU Xin<sup>1</sup>, LI Bin<sup>1</sup>, XU Hui<sup>1</sup>, YU Hong-Xi<sup>1</sup>, LI Jun<sup>1</sup>, MA Kai-Xue<sup>2</sup>, THANGARASU Bharatha Kumar<sup>3</sup>, YEO Kiat Seng<sup>2,3</sup>

- (1. Dept. of Microwave Technology, China Academy of Space Technology (Xi'an), Xi'an 710049, China;
2. School of Microelectronics, Tianjin University, Tianjin 300072, China;
3. Singapore University of Technology and Design (SUTD), Singapore 487372)

**Abstract:** This paper presents the work of a miniaturized 60-GHz balun chip with isolation and matching performance fabricated in 0.18- $\mu\text{m}$  SiGe BiCMOS process. The use of isolation circuit as key building blocks within a 60-GHz transformer balun leads to an improved isolation performance between output ports, while simultaneously achieving the matching performance of them. Moreover, compared to the conventional isolation circuit, the artificial left-handed transmission line is introduced to remove the bulky distributed elements, and the capacitive loading compensation technique is utilized for both matching and miniaturization. Both electromagnetic simulation and measurement results of the proposed 60-GHz transformer balun chip design with isolation and matching characteristics are given with good agreement. From measurement results, better than 25-dB isolation and 18-dB return loss of the output ports have been achieved at 60 GHz, with an occupied area of 0.022 mm<sup>2</sup>.

**Key words:** transformer balun, isolation circuit, 60 GHz, left-handed transmission line (LHTL)

## 基于 0.18- $\mu\text{m}$ 锗硅 BiCMOS 工艺的 60 GHz 匹配型高隔离小型化变压器巴伦

张大为<sup>1,3\*</sup>, 徐鑫<sup>1</sup>, 李斌<sup>1</sup>, 徐辉<sup>1</sup>, 于洪喜<sup>1</sup>, 李军<sup>1</sup>, 马凯学<sup>2</sup>,  
THANGARASU Bharatha Kumar<sup>3</sup>, YEO Kiat Seng<sup>2,3</sup>

- (1. 中国空间技术研究院西安分院 微波技术研究所, 中国 陕西 西安 710049;
2. 天津大学 微电子学院, 中国 天津 300072;
3. 新加坡科技设计大学, 新加坡 487372)

**摘要:** 介绍了一种工作在 60 GHz 频率的具有输出端口间高隔离和全端口匹配特性的小型化变压器巴伦芯片, 该芯片采用 0.18- $\mu\text{m}$  锗硅 BiCMOS 工艺设计并加工。通过在 60 GHz 变压器巴伦的输出端口之间引入隔离电路, 提高巴伦的隔离度性能并改善输出端口匹配性能; 在此基础上, 提出了一种基于左手材料传输线的隔离电路, 能大大改善传统隔离电路中分布式传输线尺寸大的问题; 为了进一步实现巴伦的小型化, 在设计中采用了负载电容补偿技术, 同时能改善变压器巴伦输入端口的匹配性能。设计的巴伦芯片经过电磁场仿真, 其结果与在片测试结果有较高的一致性, 验证了提出的设计方法, 设计的巴伦芯片具有全端口匹配和输出端口间高隔离度的特性。基于实测结果, 在 60 GHz 频率处, 设计的巴伦芯片实现了超过 25 dB 的输出端口隔离度和优于 18 dB 的输出端口回波损耗, 且占用尺寸极小, 仅为 0.022 mm<sup>2</sup>。

**关键词:** 变压器巴伦; 隔离电路; 60 GHz; 左手材料传输线

中图分类号: TN433

文献标识码: A

Received date: 2021-03-23, revised date: 2021-10-23

收稿日期: 2021-03-23, 修回日期: 2021-10-23

Foundation items: Supported by the National Natural Science Foundation of China (62001372).

Biography: ZHANG Da-Wei (1989-), male, Anhui China, Ph. D. Research area involves Spaceborne Microwave&Millimeter-wave MMIC and RFIC design. E-mail: qbgu@163.com.

\*Corresponding author: E-mail: qbgu@163.com

## Introduction

Baluns, which convert between unbalanced signal and balanced signal, are crucial components for various modern radio-frequency systems<sup>[1-6]</sup>. At low frequencies, baluns are commonly implemented in a flux coupling transformer form, which are known as the transformer-based balun. As frequency increases, transformer balun can be created by utilizing high-quality multi-layer metal connections provided by nowadays advanced silicon-based semiconductor technology. A transformer-based balun splitter is a three-port circuit component providing power division with out-of-phase outputs, which occupies less circuit area as compared to the widely used Wilkinson divider, making it more suitable for radio frequency integrated circuit (RFIC) design. The isolation and matching performances of balun splitter are critical, because the least interaction between the two channels before combination is expected. However, for ideal lossless balun splitters, the isolation and return loss of output ports is only 6 dB<sup>[6],[7]</sup>. This ‘ideal’ lossless isolation performance commonly exists in a conventional Marchand balun splitter; however, due to the existence of intrinsic inductance of the transformer windings, the matching performance of transformer-based balun splitter can be even worse.

To address the above issues, firstly capacitive loading compensation technique is utilized for both ‘ideal’ lossless performance and size reduction. Then, to further improve the isolation and matching performance, a distributed isolation circuit (IC) must be introduced to the transformer balun, as discussed in Ref. [7]. Circuit examples of several isolated Marchand baluns and branch-line baluns have been proposed<sup>[8],[9]</sup>. In Ref. [10], a lumped-element isolation circuit is introduced for size reduction of a balun band-pass filter. However, none of these research studies the improvement on isolation and matching performance of the transformer-based balun splitter. Therefore, in this work, we introduce the isolation circuit to a 60-GHz transformer-based balun splitter. To reduce the size caused by conventional distributed isolation circuit, a lumped isolation circuit based on artificial left-handed transmission lines (LHTLs)<sup>[11]</sup> is utilized. Moreover, design equation of the LHTL-based lumped isolation circuit is further deduced. The transformer-based balun splitter design is implemented in a commercial 0.18- $\mu\text{m}$  SiGe BiCMOS process with six metal layers, the core part occupying only 0.022- $\text{mm}^2$  area. For a 50- $\Omega$  system, measurement results show that, at 60 GHz, better than 25-dB isolation between output ports has been achieved, and the return loss is better than 18 dB.

## 1 Analysis and design of proposed transformer-based balun splitter

The proposed 60-GHz transformer-based balun splitter is designed and fabricated in 0.18- $\mu\text{m}$  SiGe BiCMOS process. Fig. 1 shows the block diagram of the proposed transformer-based balun splitter, which is composed by a

conventional transformer balun with capacitive loading compensation (CLC) technique<sup>[6]</sup> for size reduction, and an LHTL-based lumped isolation circuit placed between the two output ports to improve the isolation and matching performance.

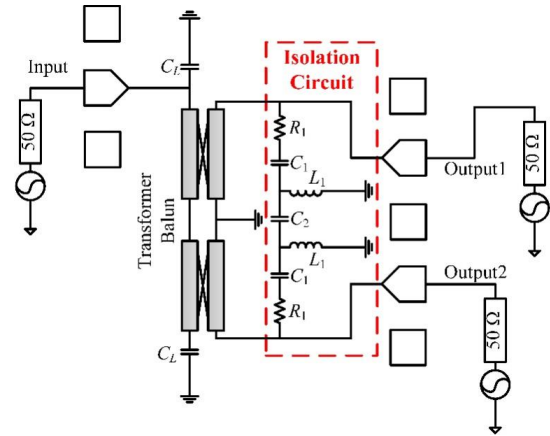


Fig. 1 Block diagram of proposed transformer-based balun splitter with isolation and matching characteristic.

图1 本文提出的匹配型高隔离变压器巴伦的原理图

### 1.1 Capacitive loading compensation technique

The proposed transformer-based balun splitter adopts two broadside-coupled couplers, as depicted in Fig. 2, where the primary and secondary vertically stacked octagonal coils are shown. There are 6 metal layers in the implemented BiCMOS process, the thickness of top metal (M6) is 2.81  $\mu\text{m}$ , while it is 1.59  $\mu\text{m}$  and 0.62  $\mu\text{m}$  for the two metal layers (M5 and M4) below M6, as shown in Fig. 2(a). M6 and M5 are adopted to build the primary windings and secondary windings respectively, while M4 is utilized as the common ground layer. The vertical metal-insulator-metal (MIM) capacitor is realized using M4 as the bottom plate and additional top plate layer, with an area capacitance of 2  $\text{fF}/\mu\text{m}^2$ . The thin film metal resistor is formed below M4 with sheet resistance of 24.5  $\Omega/\text{sq}$ .

For the proposed transformer-based balun splitter, as depicted in Fig. 2(b), the width and diameter of primary coil at top metal M6 is 6  $\mu\text{m}$  and 68  $\mu\text{m}$  respectively, while M5 is adopted to form the secondary coil with the same width and diameter. The center tap of the secondary coil is connected directly to the common ground at M4. The spacing between primary and secondary coils is 2  $\mu\text{m}$  according to the dielectric thickness of the process.

The loading capacitor  $C_L$ , as shown in Fig. 1, if being controlled properly, the length of the coupled lines of transformer balun can be reduced effectively<sup>[6]</sup>. As discussed in Ref. [6], under lossless condition, there is perfect match at the input port of the ideal three-port balun splitter. However, due to the existence of intrinsic inductance of the transformer windings, the matching performance of transformer-based balun splitter can be even worse. By introducing the CLC technique, it avoids the need to increase the transformer winding size to realize input matching performance. Therefore, CLC technique

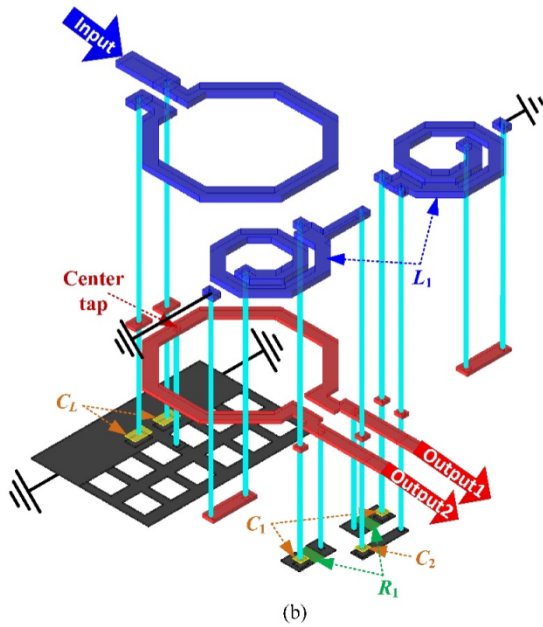
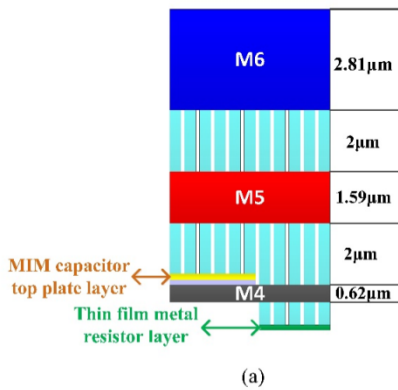


Fig. 2 Physical composition of proposed transformer-based balun splitter, (a) cross-sectional view of implemented BiCMOS back-end process, (b) three-dimensional layout representation of the proposed balun.

图2 提出的变压器巴伦的物理结构, (a) 采用的锗硅 BiCMOS 工艺的剖视图, (b) 提出的巴伦的三维结构示意图

is utilized for both input matching performance and size reduction.  $C_L$  is implemented in MIM capacitor form, with top plate connected to the primary coil ends and bottom plate connected to the common ground at M4, as illustrated in Fig. 2(b). The value of  $C_L$  is chosen to be  $103\text{ fF}$  with the size of  $5.6\ \mu\text{m} \times 9.2\ \mu\text{m}$ . In this configuration, the size of the capacitive loaded 60-GHz transformer balun structure is only about  $90\ \mu\text{m} \times 80\ \mu\text{m}$ . The capacitive loaded transformer balun is three-dimensionally modeled and simulated using Keysight's Momentum simulator, of which the results are shown in Fig. 3.

As depicted in the electromagnetic (EM) simulation results in Fig. 3, more than 15-dB input return loss has been realized at 60 GHz of the capacitive loaded transformer balun, while the isolation and return loss of the output ports is around 6.5 dB, with the size of only  $90\ \mu\text{m} \times 80\ \mu\text{m}$ . Hence, by utilizing the CLC technique, both input matching performance and size reduction of

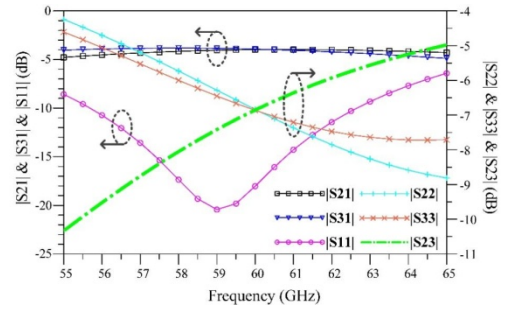


Fig. 3 Electro-magnetic simulation result of capacitive loaded transformer balun.

图3 电容负载补偿变压器巴伦的电磁场仿真结果

the transformer-based balun splitter can be achieved.

## 1.2 LHTL-based isolation circuit

Under lossless condition, the optimum scattering parameter matrix of an 'ideal balun splitter' can be written as<sup>[6]</sup>,

$$S_{ideal\ balun} \cong \begin{bmatrix} 0 & \frac{j}{\sqrt{2}} & \frac{-j}{\sqrt{2}} \\ \frac{j}{\sqrt{2}} & \frac{1}{2} & \frac{1}{2} \\ \frac{-j}{\sqrt{2}} & \frac{1}{2} & \frac{1}{2} \end{bmatrix}. \quad (1)$$

Eq. (1) reveals that the isolation and return loss performance of the output ports of an ideal balun splitter is 6 dB. To further improve the isolation and matching performance of a balun splitter, a resistive isolation circuit must be introduced. As discussed in Ref. [7], the resistive isolation circuit should be placed between the two output ports to improve the isolation and matching performance, while it is composed by a  $180^\circ$  transmission-line section and two sets of series' connection of  $R_i$  and  $C_i$ , as shown in Fig. 4(a).

In this case of the capacitive loaded transformer-based balun splitter, since its size is only  $90\ \mu\text{m} \times 80\ \mu\text{m}$ , the large size of the bulky distributed  $180^\circ$  transmission line is not acceptable. To make the balun more compact and feasible in layout routing, the bulky distributed  $180^\circ$  transmission line should be removed. In this work, a lumped LHTL-based isolation circuit is proposed for the capacitive loaded transformer-based balun splitter, of which the schematic is shown in Fig. 4.

Compared to right-handed  $180^\circ$  transmission lines, LHTLs can achieve more time delay, more phase shift and more compact design because of the larger phase constant<sup>[11]</sup>. Fig. 4(b) shows the adopted LHTL unit-cell with series' capacitance and parallel inductance connection; by cascading these LHTL cells together, certain value of phase shift can be achieved. In this design, we adopt 2 identical LHTL cells; by absorbing the series connected capacitors together as shown in Fig. 4(b), the schematic of proposed lumped isolation circuit can be further obtained as illustrated in Fig. 4(c). Based on the dispersion relation analysis of each LHTL cell in Ref. [12], the phase shift  $\Phi$  of each LHTL cell can be further

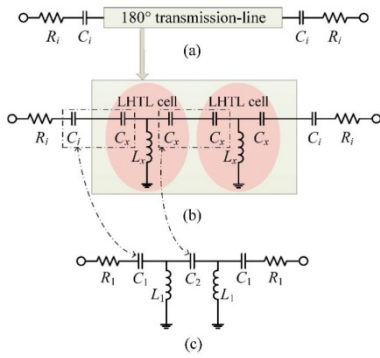


Fig. 4 Schematic of isolation circuit for baluns, (a) conventional isolation circuit, (b) cascaded LHTL-cells replacing  $180^\circ$  transmission line, (c) proposed lumped isolation circuit  
图4 巴伦的隔离电路原理图, (a) 传统隔离电路原理图, (b) 级联左手材料传输线替换  $180^\circ$  传输线, (c) 提出的集总隔离电路原理图

derived as,

$$\cos \Phi \cong 1 + ZY \quad , \quad (2)$$

where,  $Z$  and  $Y$  correspond to the series' impedance and parallel admittance of the periodic LHTL cell structure, which can be written as,

$$Z = \frac{1}{j\omega C_x} \quad , \quad (3)$$

$$Y = \frac{1}{j\omega L_x} \quad , \quad (4)$$

where  $\omega$  is the angular frequency.

By substituting Eq. (3) and Eq. (4) into Eq. (2), the phase shift of each LHTL cell can be further calculated as

$$\Phi = -\arccos \left( 1 - \frac{1}{\omega^2 L_x C_x} \right) \quad . \quad (5)$$

To realize the  $180^\circ$  phase shift at 60 GHz, as well considering the implemented process,  $L_x$  and  $C_x$  are chosen to be  $116\text{pH}$  and  $61\text{fF}$ , respectively. From Eq. (5), the phase shift of each cell can be obtained as  $89.7^\circ$ ; by cascading two of the identical LHTL cells as shown in Fig. 4(b), about  $180^\circ$  phase shift can be realized. The phase shift and insertion loss performance of the 2 cascaded LHTL-cells are simulated under  $50\text{-}\Omega$  termination, and comparison is made with the simulated performance of a thin-film micro strip  $180^\circ$  transmission line using the same process, as shown in Fig. 5.

The thin film micro strip  $180^\circ$  transmission line is created by utilizing M4 as ground layer and M6 as signal layer. In this configuration, the line width of the  $180^\circ$  transmission line can be calculated as  $6\mu\text{m}$  and the line length is  $1450\mu\text{m}$ ; as a comparison, it has a much more compact size of the 2 cascaded LHTL-cells, which is only  $160\mu\text{m} \times 50\mu\text{m}$ . As revealed from Fig. 5, close to  $180^\circ$  phase shift and 0 dB insertion loss performance can be achieved of both cascaded LHTL-cells and  $180^\circ$  transmission line at 60 GHz, which means that the cascaded LHTL-cells can be well-implemented for the isolation circuit.

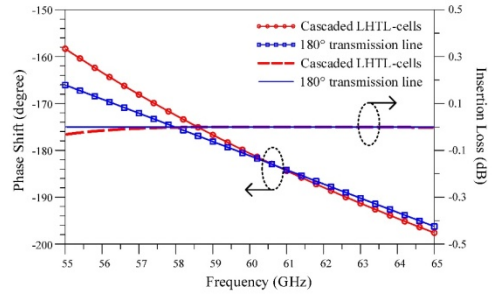


Fig. 5 Performance comparison between cascaded LHTL-cells and  $180^\circ$  transmission line

图5 级联左手材料单元和  $180^\circ$  传输线性能对比

Therefore, with the proposed cascaded LHTL-cells for the isolation circuit design, miniaturization of transformer-based balun splitter with isolation and matching performance can be enabled.

Based on the analysis above, the value of each circuit component can be calculated as,  $L_1 = L_x = 116\text{pH}$ ,  $C_2 = C_x/2 = 30.5\text{fF}$ ,  $C_1 = C_x \cdot C_i / (C_x + C_i)$ ,  $R_1 = R_i$ . By taking the lumped components into co-simulation with the capacitive loaded transformer balun, the value of  $R_1$  and  $C_1$  can be further determined as,  $R_1 = 17\Omega$ ,  $C_1 = 35\text{fF}$ . Then, the lumped LHTL-based isolation circuit is connected to the two output ports of capacitive loaded transformer balun as shown in Fig. 1, and the three-dimensional structure of the designed transformer-based balun splitter is illustrated in Fig. 2(b).

## 2 Experimental results

The proposed transformer-based balun splitter has been designed and checked by performing EM simulations using Keysight Momentum simulator, before fabrication in a commercial  $0.18\text{-}\mu\text{m}$  BiCMOS technology. The measurement setup and die photograph of the designed transformer-based balun splitter are shown in Fig. 6. The core part of the proposed balun splitter occupies only  $160\mu\text{m} \times 140\mu\text{m}$ . The fabricated transformer balun die is measured by using a Keysight N5247A 4-port vector network analyzer (VNA), together with Cascade probe station and RF probes. The additional on-chip 4<sup>th</sup> port is only for measurement use and directly connected to the on-chip ground. The 3-port S-parameter data of the fabricated balun can be further obtained from the VNA's 4-port measurement result. The designed transformer-based balun splitter is measured under a  $50\text{-}\Omega$  system, of which the comparison result between measurement and simulation is shown in Fig. 7.

At 60 GHz, the measured isolation performance between output ports is more than 25 dB, and the return loss of the output ports is better than 18 dB. From 55 GHz to 65 GHz, the isolation and return loss of the output ports are better than 15 dB and 10 dB, respectively. Fig. 7(b) displays the measured insertion loss, amplitude and phase imbalance versus frequency. The amplitude and phase imbalance performance is expressed in terms of the amplitude difference between S21 and S31, and phase difference with reference to  $180^\circ$  of S21 and



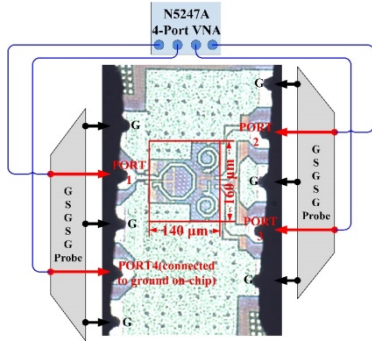


Fig. 6 Measurement setup and die photograph of designed balun splitter.

图6 在片测试设置和设计的巴伦芯片照片

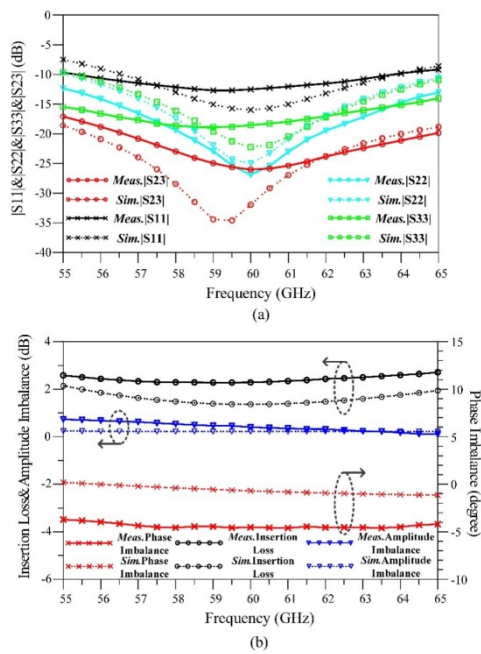


Fig. 7 Measurement results comparison of the fabricated balun splitter chip (a) isolation and return loss result from measurement and simulation, (b) insertion loss and imbalance result from measurement and simulation

图7 设计的巴伦芯片的实测数据对比 (a) 仿真和在片实测的隔离度和回波损耗结果对比, (b) 仿真和在片实测的插入损耗和不平衡度特性结果对比

S31 as proposed in Ref. [6]. The insertion loss is the average loss value of S21 and S31 excluding the 3-dB theoretical loss. The measured insertion loss is better than

2.7 dB, while the amplitude and phase imbalance are better than 0.8 dB and  $5^\circ$  respectively, within the frequency range of 55 GHz to 65 GHz. As compared with the state-of-the-art designs summarized in Table I, more than 25-dB isolation of the transformer balun is firstly achieved at 60 GHz, with only 0.022- $\text{mm}^2$  compact size.

### 3 Conclusions

This paper presents a miniaturized 60-GHz transformer-based balun splitter chip with isolation and matching characteristic. With the proposed LHTL-based isolation circuit, isolation and matching performance can be achieved of the transformer balun, compact size can be maintained as well. The fabricated balun splitter achieves a compact chip area of 0.022  $\text{mm}^2$  and more than 25-dB isolation at 60 GHz. Good agreement on simulation and measurement indicates positive research value in realizing compact balun splitter chip, and to be applied in future millimeter-wave highly integrated systems.

### Acknowledgment

This work was supported by the National Natural Science Foundation of China (Grant No. 62001372). The authors would like to thank the Tower Jazz team for their help in the fabrication, and Dr. Lu Muting from Singapore University of Technology and Design for her help in the on-chip measurement.

### References

- [1] Chakraborty S, Milner L E, Hall L T, *et al.* A 30 - 60 GHz SiGe transformer balun with offset radii coils for low amplitude and phase imbalance [C]. In 2017 IEEE MTT-S International Microwave Symposium (IMS) Digest. Hawaii, 2017: 1278-1281.
- [2] Yang G, Wang K, Wang Z. 20.8 - 51 GHz highly balanced CMOS balun [J]. *Electronics Letters*, 2017, **53**(17): 1202-1203.
- [3] Hsu C Y, Chen C Y, Chuang H R. A 77-GHz CMOS on-chip band-pass filter with balanced and unbalanced outputs [J]. *IEEE Electron Device Letters*, 2010, **31**(11): 1205-1207.
- [4] Zhang D, Yu H, Kumar T B, *et al.* Design of millimeter-wave transformer balun with isolation circuit in silicon-based technology [C]. 2016 International Symposium on Integrated Circuits (ISIC). Singapore, 2016: 1-3.
- [5] Lei-Jun X, Bo H, Xue B, *et al.* Modeling and design of millimeter-wave Marchand balun based on three-conductor coupled line [J]. *J. Infrared Millim. Waves*, (徐雷钧, 黄波, 白雪, 等. 基于三导体耦合线的毫米波 Marchand balun 建模与设计. *红外与毫米波学报*) 2015, **34**(6): 705-709.
- [6] Ma K, Yan N, Yeo K S, *et al.* Miniaturized 40 - 60 GHz on-chip balun with capacitive loading compensation [J]. *IEEE Electron Device Letters*, 2014, **35**(4): 434-436.
- [7] Ahn H R, Itoh T. New isolation circuits of compact impedance-transforming 3-dB baluns for theoretically perfect isolation and matching

Table 1 Performance summary of reported 60-GHz on-chip balun splitter

表1 已发表的60-GHz在片巴伦性能总结对比

Reference	Topology	Band (GHz)	Isolation (dB)	Output return loss (dB)	Insertion loss (dB)	Phase error ( $^\circ$ )	Amplitude error (dB)	Size ( $\text{mm}^2$ )
[1]	Transformer	30-60	N. A.	N. A.	<3	< $\pm 1$	<0.2	0.029
[2]	Marchand	20.8-51	N. A.	N. A.	<2	< $\pm 2$	<0.3	0.042
[6]	Transformer+CLC	40-60	N. A.	N. A.	2~2.4	<2.7	<0.2	0.036
[8]	Marchand+IC	25-65	N. A.	>13@60 GHz	<7	< $\pm 10$	<2	0.55
This work	Transformer+CLC+IC	55-65	>25@60 GHz	>18@60 GHz	2.3~2.7	4.4~4.8	<0.8	0.022

- [J]. *IEEE Transactions on Microwave Theory and Techniques*, 2010, **58**(12): 3892–3902.
- [8] Liu C H, Hsu C Y, Chuang H R, *et al.* A 60-GHz millimeter-wave CMOS Marchand balun using 0.18- $\mu\text{m}$  CMOS technology [J]. *Microwave and Optical Technology Letters*, 2009, **51**(3): 766–770.
- [9] Kim P, Chaudhary G, Jeong Y. Unequal termination branch-line balun with high-isolation wideband characteristics [J]. *Microwave and Optical Technology Letters*, 2016, **58**(8): 1775–1778.
- [10] Yang T, Chi P L, Itoh T. Lumped isolation circuits for improvement of matching and isolation in three-port balun band-pass filter [C]. In 2010 IEEE MTT-S International Microwave Symposium (IMS) Digest. Anaheim, 2010: 584–587.
- [11] Zhang D, Xu X, Yu H, *et al.* Predistortion linearizer for wideband AM/PM cancelation with left-handed delay line [J]. *IEEE Microwave and Wireless Components Letters*, 2017, **27**(9): 794–796.
- [12] Eleftheriades G V, Iyer A K, Kremer P C. Planar negative refractive index media using periodically LC loaded transmission lines [J]. *IEEE Transactions on Microwave Theory and Techniques*, 2002, **50**(12): 2702–2712.